JB
Journals.ASM.org

Resuscitation-Promoting Factors Are Cell Wall-Lytic Enzymes with Important Roles in the Germination and Growth of *Streptomyces coelicolor*

Danielle L. Sexton, Renée J. St-Onge, Henry J. Haiser, Mary R. Yousef, Lauren Brady, Chan Gao, Jacqueline Leonard, Marie A. Elliot

Department of Biology and M. G. DeGroote Institute for Infectious Disease Research, McMaster University, Hamilton, Ontario, Canada

Dormancy is a common strategy adopted by bacterial cells as a means of surviving adverse environmental conditions. For *Streptomyces* bacteria, this involves developing chains of dormant exospores that extend away from the colony surface. Both spore formation and subsequent spore germination are tightly controlled processes, and while significant progress has been made in understanding the underlying regulatory and enzymatic bases for these, there are still significant gaps in our understanding. One class of proteins with a potential role in spore-associated processes are the so-called resuscitation-promoting factors, or Rpfs, which in other actinobacteria are needed to restore active growth to dormant cell populations. The model species *Streptomyces coelicolor* encodes five Rpf proteins (RpfA to RfpE), and here we show that these proteins have overlapping functions during growth. Collectively, the *S. coelicolor* Rpfs promote spore germination and are critical for growth under nutrient-limiting conditions. Previous studies have revealed structural similarities between the Rpf domain and lysozyme, and our *in vitro* biochemical assays revealed various levels of peptidoglycan cleavage capabilities for each of these five *Streptomyces* enzymes. Peptidoglycan remodeling by enzymes such as these must be stringently governed so as to retain the structural integrity of the cell wall. Our results suggest that one of the Rpfs, RpfB, is subject to a unique mode of enzymatic autoregulation, mediated by a domain of previously unknown function (DUF348) located within the N terminus of the protein; removal of this domain led to significantly enhanced peptidoglycan cleavage.

Streptomyces species are Gram-positive bacteria that abound in soil environments. They are renowned for their secondary metabolic capabilities; they produce a multitude of compounds that have found utility in both medicine and agriculture, including a vast array of antibiotics, chemotherapeutics, immunosuppressants, and antiparasitic agents (1). They are also well known for their complex, multicellular developmental cycle (2). The *Streptomyces* life cycle can be broadly divided into two stages: vegetative growth and reproductive development. Unlike most bacteria, *Streptomyces* organisms are filamentous, and during the vegetative phase of their life cycle, they grow by hyphal tip extension and branching, ultimately forming an interwoven network of cells known as the vegetative mycelium (3). Under certain as yet poorly defined stress conditions, vegetative growth ceases, and reproductive growth ensues. Here, unbranched filamentous cells, termed aerial hyphae, grow away from the vegetative mycelium and extend into the air. These cells then undergo a synchronous round of chromosome segregation, cell division, and cell wall modification to yield chains of dormant exospores (4). These spores are resistant to a wide variety of environmental insults and can be widely dispersed.

A dormant cell state is not unique to the streptomycetes, and indeed many well-studied bacteria (e.g., *Bacillus*, *Clostridium*, and *Myxococcus*) have adopted sporulation as a means of surviving adverse environmental conditions (5). Other bacteria have evolved less extreme dormant states and instead adopt cell states with low metabolic activity such that these cells are better able to tolerate stresses such as antibiotic exposure or immune system assault (6). In addition to low metabolic activity, dormant cells of all types often have a cell wall architecture that differs from that of their vegetative counterparts. For example, *Bacillus* spores possess thick cell walls comprising peptidoglycan with altered cross-linking compared with that of vegetative cells (7). Similarly, latent or dormant *Mycobacterium tuberculosis* cells display a different cell wall structure relative to that of actively growing cells (8).

While a thick wall constitutes an effective protective barrier, it can also be refractory to cell growth. Consequently, cell wall remodeling must be integral to restoring dormant cells to an active growth state. In the actinobacteria, a group that includes both the mycobacteria and the streptomycetes, a protein family dubbed the resuscitation-promoting factors (Rpfs) have been implicated in the cleavage of dormant cell walls and subsequent promotion of growth and metabolic reactivation (9). The first Rpf protein was identified in *Micrococcus luteus*, an actinobacterium that forms dormant cells following prolonged starvation. In an elegant set of experiments, Mukamolova and colleagues found that picomolar concentrations of this secreted protein were sufficient to convert dormant *Micrococcus* cells into actively growing cells (10, 11). Intriguingly, the Rpf protein in *M. luteus* is essential for viability

Received 31 October 2014 **Accepted** 9 December 2014

Accepted manuscript posted online 15 December 2014

Citation Sexton DL, St-Onge RJ, Haiser HJ, Yousef MR, Brady L, Gao C, Leonard J, Elliot MA. 2015. Resuscitation-promoting factors are cell wall-lytic enzymes with important roles in the germination and growth of *Streptomyces coelicolor*. J Bacteriol 197:848–860. doi:10.1128/JB.02464-14.

Editor: P. J. Christie

Address correspondence to Marie A. Elliot, melliot@mcmaster.ca.

Supplemental material for this article may be found at http://dx.doi.org/10.1128/JB.02464-14.

doi:10.1128/JB.02464-14

(11), suggesting that its function may extend beyond dormant cell resuscitation. Subsequent studies have focused on the Rpf proteins in *Mycobacterium*; *M. tuberculosis* encodes five Rpf (Rpf_{MTB}) proteins (12). These proteins share some functional redundancy (13), and while it is possible to delete all five *rpf* genes without affecting viability, the corresponding mutant is unable to exit dormancy and is further compromised in its ability to initiate/establish infections in mouse models (14–16). Several Rpfs in the mycobacteria appear to act as part of a larger peptidoglycan cleavage complex, associating with RipA, an essential enzyme with endopeptidase activity (17, 18).

The mechanistic basis underlying Rpf-mediated emergence from dormancy has not been fully elucidated. An important step toward understanding Rpf activity came with the solution structure of the Rpf domain from RpfB of *M. tuberculosis*, which revealed a protein fold with similarity to both lysozyme and lytic transglycosidases (19). These results suggested that proteins with an Rpf domain may cleave within the polysaccharide backbone of the peptidoglycan. Given this predicted activity, two—not mutually exclusive—hypotheses have been put forward to explain how Rpf proteins could promote exit from dormancy: (i) Rpf activity relieves the physical constraints imposed by the altered cell wall structure that had otherwise inhibited growth of the dormant cell; (ii) Rpf activity serves as a signal (or generates a signal) that is, in turn, sensed by the cell, and this signal stimulates the resumption of growth (9).

Like *M. tuberculosis*, the best-studied streptomycete, *Streptomyces coelicolor*, encodes five Rpf (Rpf_{SC}) proteins (20). Generally speaking, these proteins are not orthologous to the *M. tuberculosis* proteins, with only one of the five (RpfB) sharing a similar domain organization. Here, we probe the role of these proteins in the growth and development of *S. coelicolor*, compare their peptidoglycan cleavage capabilities and interaction potential, and uncover an intriguing modulatory role for a domain of unknown function associated with RpfB.

MATERIALS AND METHODS

Bacterial strains and culture conditions. Bacterial strains used or created in this work are detailed in Table 1. *S. coelicolor* A3(2) strain M145 and its derivatives were grown at 30°C on R5, mannitol soya flour (MS), Difco nutrient agar (NA), or LB agar medium supplemented with antibiotics to maintain selection where appropriate, or in either a 50:50 mixture of tryptic soy broth–yeast extract-malt extract (TSB-YEME) liquid medium or liquid new minimal medium with phosphate (NMMP), as described by Kieser et al. (21). All *Escherichia coli* strains were grown at 37°C on LB or NA agar plates or in LB or super optimal broth (SOB) liquid medium, supplemented with antibiotics where appropriate, with the exception of BW25113, which was grown at 30°C. All *Saccharomyces cerevisiae* strains were grown at 30°C in yeast-peptone-dextrose-adenine (YPDA) liquid medium or on YPDA or synthetic defined (SD) amino acid drop-out agar plates (Clonetech) to maintain selection where appropriate.

Total RNA isolation. *S. coelicolor* M145 was grown at 30°C on MS agar plates overlaid with cellophane discs. At different developmental stages (vegetative growth, aerial development, and early and late sporulation), biomass was harvested using a sterile spatula. M145 was also grown at 30°C in TSB-YEME medium, and cells were recovered from culture aliquots by centrifugation. Samples were frozen at −80°C for 3 to 6 days. Total RNA was extracted by mechanical disruption, and coextracted DNA was digested using Turbo DNase (Ambion), as previously described by Moody et al. (22). Total RNA was quantified using a NanoDrop ND-1000, and RNA integrity was confirmed by size fractionating 2 μg of total RNA on an agarose gel. RNA extract purity was verified by measuring the A_{260}/A_{280} and A_{260}/A_{230} ratios; these ranged from 1.88 to 2.03 and from 2.18 to 2.38, respectively.

Primer design for reverse transcription-quantitative PCR (RT-qPCR) analyses. The predicted *rpfA* (*SCO3097*), *rpfB* (*SCO3150*), *rpfC* (*SCO3098*), *rpfD* (*SCO0974*), and *rpfE* (*SCO7458*) coding sequences were retrieved from the *Streptomyces* annotation server StrepDB (http://strepdb.streptomyces.org.uk/). Gene-specific PCR primers, generating products of 50 to 150 nucleotides (nt), were designed using Primer-BLAST (http://www.ncbi.nlm.nih.gov/tools/primer-blast/) (see Table S1 in the supplemental material). Standard desalted primers were purchased from Integrated DNA Technologies.

The specificity of each primer pair to its intended target was tested *in silico* by searching the *S. coelicolor* genome for potential product-generating annealing sites. Generation of a single amplicon was confirmed by PCR. Briefly, 20-μl reaction mixtures contained 1× *Taq* reaction buffer, 200 μM each deoxynucleoside triphosphate (dNTP), 5% (vol/vol) dimethyl sulfoxide, 300 nM each primer (see Table S1 in the supplemental material), 0.125 U/μl *Taq* DNA polymerase, and 1 ng/μl *S. coelicolor* M145 genomic DNA. Nuclease-free water was used as the template for the negative-control reactions. The following amplification conditions were used: initial denaturation at 95°C for 3 min; 35 amplification cycles consisting of denaturation at 95°C for 30 s, annealing for 30 s (temperatures were optimized for each primer pair) (see Table S1), and extension at 72°C for 45 s, followed by a final extension step at 72°C for 5 min.

Reverse transcription and real-time PCR. *rpfA*, *rpfB*, *rpfC*, *rpfD*, and *rpfE* transcripts were reverse transcribed using SuperScript III reverse transcriptase (Invitrogen). An initial reaction mixture containing 167 ng/μl total RNA, 167 nM each reverse primer, and 833 μM each dNTP (Fermentas or Invitrogen) was heated at 95°C for 5 min and immediately cooled on ice. Each reaction mixture was then supplemented with a second solution containing 2.5× First-Strand buffer (Invitrogen), 12.5 mM dithiothreitol, 5 U/μl RNaseOUT (Invitrogen), and 25 U/μl SuperScript III reverse transcriptase (RT) (Invitrogen). Transcripts were reverse transcribed at 55°C for 60 min, prior to heat inactivation of the enzymes at 70°C for 15 min. To verify the absence of undigested genomic DNA, no-RT controls were conducted as described above, except that RNaseOUT and SuperScript III reverse transcriptase were omitted. The resulting cDNA samples were stored at −20°C for no more than 5 days.

cDNA was quantified using real-time PCR. Triplicate 20- or 25-μl singleplex reactions were carried out in 1× PerfeCTa SYBR green SuperMix (Quanta Biosciences), together with 300 nM each gene-specific primer and 8 ng/μl reverse-transcribed total RNA. No-template negative controls, in which cDNA was replaced with an equal volume of nuclease-free water, were included in each PCR run. Reactions were performed in clear 96-well PCR plates (Bio-Rad) with a CFX96 Touch Real-Time PCR detection system (Bio-Rad) under the following conditions: initial denaturation at 95°C for 3 min, followed by 50 amplification cycles consisting of denaturation at 95°C for 15 s and annealing/extension at a primer-specific temperature (see Table S1 in the supplemental material) for 45 s. Fluorescence was measured during each extension step. A melt curve analysis (65 to 95°C with 5-s fluorescence reads every 0.5°C increase) was also conducted immediately following product amplification.

Fluorescence data were baseline corrected using CFX Manager software, version 2.1 (Bio-Rad). Transcript levels were then calculated using the DART-PCR, version 1.0 workbook (23). Starting fluorescence values (R_0), which are proportional to initial template quantities, were calculated for each sample using the average midpoint and amplification efficiency for a given primer pair, as described by Peirson et al. (23). Expression levels of each gene were normalized to total RNA mass and PCR product length.

Luciferase assays. To monitor *rpf* expression during germination, the promoter regions for each *rpf* gene were cloned into the BamHI and KpnI sites of pFLUX (Table 1; see also Table S2 and Fig. S1 in the supplemental material), and these constructs, together with pFLUX alone (negative control) and pFLUX plus the *ermE** promoter (positive control, where

TABLE 1 Plasmids and *Streptomyces coelicolor*, *Escherichia coli*, and *Saccharomyces cerevisiae* strains

Strain or plasmid	Genotype, characteristic(s), and/or use[a]	Reference or source
Streptomyces coelicolor A3(2) strains		
M145	SCP1$^-$ SCP2$^-$	21
E104	M145 *SCO3097*::*aac(3)IV*	25
E104a (Δ*rpfA*)	M145 Δ*SCO3097*	This study
E110 (Δ*rpfC*)	M145 *SCO3098*::*aac(3)IV*	This study
E111 (Δ*rpfB*)	M145 *SCO3150*::*vph*	This study
E112 (Δ*rpfD*)	M145 SCO0974::TOPO 2.1	This study
E113 (Δ*rpfE*)	M145 SCO7458::*aac(3)IV*	This study
E114 (Δ*rpfAB*)	M145 *SCO3097-SCO3098*::*aac(3)IV*	This study
E114a	M145 Δ*SCO3097-SCO3098*	This study
E115 (Δ*rpfA* D*rpfB D*r*pfC*) (3× mutant)	E114a *SCO3150*::*vph*	This study
E116	E115 *SCO7458*::*aac(3)IV*	This study
E116a (Δ*rpfA D*r*pfB D*r*pfC D*r*pfE*) (4× mutant)	E115 Δ*SCO7458*	This study
E117 (Δ*rpfA* Δ*rpfB* Δ*rpfC* Δ*rpfD* Δ*rpfE*) (5× mutant)	E116a *SCO0974*::TOPO 2.1	This study
Escherichia coli strains		
DH5α	Used for routine cloning	
ET12567(pUZ8002)	*dam dcm*; with transmobilizing plasmid pUZ8002	42, 43
Rosetta 2	Protein overexpression	Novagen
BW25113	Construction of cosmid-based knockouts	44
BT340	DH5α-carrying pCP20, used for FLP recombinase-mediated removal of disruption cassettes	44
Saccharomyces cerevisiae strains		
Y2H Gold	*MAT***a** *trp1-901 leu2-3,112 ura3-52 his3-200 gal4*Δ *gal80*Δ *LYS2*::*GAL1*$_{UAS}$-*Gal1*$_{TATA}$-*His3 GAL2*$_{UAS}$-*Gal2*$_{TATA}$-*Ade2URA3*::*MEL1*$_{UAS}$-*Mel1*$_{TATA}$ *AUR1-C MEL1*	Clontech
Y187	*MAT*α *ura3-52 his3-200 ade2-101 trp1-901 leu2-3,112 gal4*Δ *gal80*Δ *met*$^-$ *URA3*::*GAL1*$_{UAS}$-*Gal1*$_{TATA}$-*LacZ MEL1*	Clontech
Plasmids		
StE41	Cosmid used for knockout of *rpfA* and *rpfC*	45
StE87	Cosmid used for knockout of *rpfB*	45
St5C11	Cosmid used for knockout of *rpfE*	45
pIJ82	pSET152 derivative, *hyg* replacing *aac(3)IV*	Gift from H. Kieser
pMC175	pIJ82 carrying *rpfD*	This work
pMC176	pIJ82 carrying *rpfE*	This work
pET15b	Overexpression of His$_6$-tagged proteins	Novagen
pMC177	pET15b carrying *rpfA*	25
pMC178	pET15b carrying *rpfB*	This work
pMC179	pET15b carrying *rpfB*Δ*DUF348*	This work
pMC180	pET15b carrying *rpfC*	This work
pMC181	pET15b carrying *rpfD*	This work
pMC182	pET15b carrying *rpfE*	This work
pGAD T7 AD	Used to generate transcriptional fusions to the GAL4 transcriptional activation domain	Clontech
pMC183	pGAD carrying *rpfA*	This work
pMC184	pGAD carrying *rpfB*	This work
pMC185	pGAD carrying *rpfB*Δ*DUF348*	This work
pMC186	pGAD carrying *rpfC*	This work
pMC187	pGAD carrying *rpfD*	This work
pMC188	pGAD carrying *rpfE*	This work
pGBK T7 BD	Used to generate transcriptional fusions to the GAL4 DNA binding domain	Clontech
pMC189	pGBK carrying *rpfA*	This work
pMC190	pGBK carrying *rpfB*	This work
pMC191	pGBK carrying *rpfB*Δ*DUF348*	This work
pMC192	pGBK carrying *rpfC*	This work
pMC193	pGBK carrying *rpfD*	This work
pMC194	pGBK carrying *rpfE*	This work
pFLUX	Integrative transcriptional reporter vector; *ori* (pUC18) *oriT* (RK2) *int* ϕBT1 *attP* ϕBT1 *luxCDABE* (promoterless) *aac(3)IV*	32
pFLUX-Pos	pFLUX carrying the *ermE** promoter	This work
pMC195	pFLUX carrying the *rpfA* promoter	This work
pMC196	pFLUX carrying the *rpfB* promoter (upstream of *SCO3152*)	This work
pMC197	pFLUX carrying the *rpfC* promoter	This work
pMC198	pFLUX carrying the *rpfD* promoter	This work
pMC199	pFLUX carrying the *rpfE* promoter	This work

[a] UAS, upstream activation sequence.

*ermE** is a constitutive, highly active promoter) (Table 1), were conjugated into wild-type *S. coelicolor* M145. Equal numbers of spores were inoculated into 150 μl of TSB-YEME liquid medium in white 96-well plates (Thermo-Fisher). Plates were then incubated at 30°C with shaking, and luminescence was measured (integration time of 4,000 ms) every 10 min for 12 h using a Tecan Ultra Evolution plate reader. Luminescence levels of the negative control were subtracted from those of the *rpf* fusions and positive control. Eight biological replicates were prepared, and experiments were conducted at least twice.

***rpf* mutant strain construction.** Single null mutations were made in *rpfB*, *rpfC*, and *rpfE* using ReDirect technology (24); the *rpfA* mutation had been created previously (25). *rpfB* was replaced with a viomycin resistance (*vph*) cassette on cosmid StE87, whereas *rpfC* and *rpfE* were each replaced with apramycin resistance [*aac(3)IV*] cassettes on cosmids StE41 and St5C11, respectively (Table 1 gives plasmid and strain information; see Table S2 in the supplemental material for primer information). For mutation of *rpfD*, the typical ReDirect gene replacement protocol was unsuccessful due to spurious cosmid recombination, and instead *rpfD* was disrupted in the chromosome. A 700-bp region encompassing the Rpf domain of *rpfD* was amplified and cloned into the TOPO vector (Invitrogen). The kanamycin resistance gene on the TOPO vector backbone was then replaced with an *aac(3)IV-oriT*-containing DNA fragment using the ReDirect protocol (24).

Mutant cosmids/disruption plasmids were introduced into the nonmethylating *E. coli* strain ET12567/pUZ8002 prior to conjugation into *S. coelicolor* M145. Resulting exconjugants were subsequently screened for double-crossover recombinants (or in the case of the *rpfD* disruption, selected for single-crossover recombinants). Correct replacement of each *rpf* gene with the appropriate antibiotic resistance cassette or, for *rpfD*, disruption of the coding sequence, was confirmed using diagnostic PCRs with mutant chromosomal DNA as the template, alongside wild-type chromosomal DNA and mutant cosmids (where appropriate) as negative and positive controls, respectively. These reactions were conducted to confirm that the cosmids/plasmids had recombined at the appropriate positions in the chromosome and that the wild-type gene was no longer present or intact (see Table S2 in the supplemental material for primer combinations).

To create markerless mutants and to permit recycling of the *aac(3)IV* resistance marker when multiple mutations were created, the apramycin resistance cassette was removed from the *rpfA rpfC* double mutant cosmid and from the *rpfE* single mutant cosmid using the temperature-sensitive FLP recombination plasmid in *E. coli* DH5α (strain BT340) (Table 1). Cosmids were introduced into these cells and grown nonselectively at 42°C to stimulate expression of the FLP recombinase. To identify colonies carrying cosmids in which the antibiotic resistance marker had been excised by FLP recombinase, colonies were tested for kanamycin resistance and apramycin sensitivity. Diagnostic PCR using primers specific for regions upstream and downstream of the Rpf coding sequences (see Table S2 in the supplemental material) was used to confirm appropriate removal of the apramycin cassette from the cosmid. These cosmids were then reintroduced into their corresponding marker-containing *S. coelicolor* mutant strain by protoplast transformation. The kanamycin-resistant transformants were then grown nonselectively and subsequently screened for double-crossover recombination and loss of both kanamycin and apramycin resistance markers; this was confirmed by PCR.

To create a multiple *rpf* mutant strain, we used the approach detailed in the schematic diagram in Fig. S2 in the supplemental material. The *rpfA rpfC* double mutant was created by replacing both genes (which are adjacent on the *S. coelicolor* chromosome) with the *aac(3)IV* resistance gene on cosmid StE41. This resistance gene was then removed, and the *rpfB*::*vph* mutant cosmid was next introduced, followed by screening and confirmation of the *rpfB* mutation as described above. Next, the *rpfE*::*aac(3)IV* mutant cosmid was introduced, and the *rpfE* mutation was confirmed before the apramycin resistance cassette was removed from *rpfE*, as outlined previously. Finally, the *rpfD* disruption construct was introduced into a mutant strain with deletions of *rpfA*, *rpfB*, *rpfC*, and *rpfE* (the 4× Δ*rpf* mutant), selected for integration into *rpfD* in the chromosome, and confirmed by PCR.

***rpf* mutant strain complementation.** Within the single *rpf* mutations, the greatest phenotypic effects were seen for *rpfA*, *rpfD*, and *rpfE* mutant strains, with the *rpfA* mutant phenotype having been complemented previously (25). To ensure that the mutant phenotypes associated with the Δ*rpfD* and Δ*rpfE* strains were due to loss of their respective Rpf proteins, complementation clones were generated. The *rpfD* coding sequence was amplified, together with sufficient upstream and downstream sequence so as to encompass all necessary regulatory elements (325 nt upstream and 244 nt downstream of the coding sequence). This fragment was then cloned into the integrating plasmid pIJ82 (Table 1), and the integrity of the resulting construct was confirmed by sequencing. The plasmid was subsequently introduced into the Δ*rpfD* mutant strain, where hygromycin-resistant colonies were selected. Complementation of *rpfE* followed a similar scheme, only the complementing fragment extended 175 bp upstream of the translation start site and 237 bp downstream of the stop codon. Empty plasmid vectors were also introduced into each mutant strain as a control for any plasmid-specific effects. Complementation was confirmed by comparing germination profiles of plasmid alone-containing mutant and wild-type strains with that of the complemented mutant strain, as described below.

TEM. Wild-type and mutant strains were grown on MS agar at 30°C for 7 days before being examined by transmission electron microscopy (TEM). TEM was performed as described by Haiser et al. (25). Images were processed using Adobe Photoshop Elements 11 Editor. Cell wall thickness was measured using ImageJ software (26) for a minimum of 25 spores per strain.

Spore germination assay. Mutant and wild-type spores were plated on MS agar overlaid with cellophane discs and incubated at 30°C for up to 12 h. At intermediate time points, a 1-cm square was excised from the cellophane disc and was examined using phase-contrast microscopy to score germinated spores (those possessing at least one germ tube) versus nongerminated spores. A minimum of 200 spores were counted per strain per time point in at least three independent experiments.

Antibiotic sensitivity assays. Two million wild-type and mutant spores were spread over 500 μl of MS agar containing bacitracin (Bioshop Canada) or D-cycloserine (Sigma-Aldrich) in 48-well microplates (Thermo-Fisher). Plates were incubated for 4 days at 30°C. For overlay experiments, spores were inoculated on 500 μl of MS agar in 48-well microplates and incubated at 30°C for 16 h (to allow for complete spore germination) before wells were overlaid with the indicated amounts of bacitracin or D-cycloserine. Plates were then incubated for an additional 3 days at 30°C. The experiment was repeated at least three times.

Protein overexpression and purification. To assess the enzymatic activity of each Rpf, the sequence encoding the extracellular domain of each protein (excluding the SignalP-predicted signal peptide sequence [27]) was amplified from *S. coelicolor* M145 chromosomal DNA using the primers described in Table S2 in the supplemental material. The amplified products were sequentially digested with BamHI and NdeI and ligated with pET15b (Novagen), which had been digested with the same enzymes and dephosphorylated prior to ligation. All constructs were verified by sequencing using promoter and terminator primers (see Table S2) before being introduced into chemically competent *E. coli* Rosetta 2 cells (Novagen). The resulting colonies were grown overnight in 5-ml cultures supplemented with ampicillin and chloramphenicol, and these overnight cultures were then used to inoculate 500 ml of LB medium containing ampicillin and chloramphenicol. Cultures were grown at 37°C to an optical density at 600 nm (OD_{600}) of 0.8, at which point isopropyl-β-D-thiogalactopyranoside (IPTG) was added in the amounts indicated in Table S3 in the supplemental material to induce protein overexpression. Cultures were incubated for the times/temperatures indicated in Table S3 before cells were collected by centrifugation.

Cell pellets were resuspended in 10 ml of lysis buffer (50 mM

NaH_2PO_4, 300 mM NaCl, 10 mM imidazole, 1 mg/ml lysozyme, pH 8.0) containing one Complete Mini EDTA-free protease inhibitor pellet (Roche) and incubated on ice for 30 min. The cell suspension was sonicated on ice six times for 10 s each before being treated with 40 μg of RNase A and 20 U of Turbo DNase (Ambion) for 15 min on ice. The lysate was then centrifuged at 10,000 × *g* for 30 min at 4°C. The supernatant was removed and incubated with 1 ml of Ni-nitrilotriacetic acid (NTA) slurry (Qiagen) for 1.5 h at 4°C before being applied to a PolyPrep chromatography column (Bio-Rad). The column was washed with buffer (50 mM NaH_2PO_4, 300 mM NaCl, pH 8.0) containing increasing concentrations of imidazole (4 ml each of wash buffer containing 20 mM, 50 mM, and 70 mM imidazole) before His_6-tagged proteins were eluted with imidazole-containing buffer at concentrations optimized for each protein (see Table S3 in the supplemental material). Purified proteins were applied to an Ultra Centricon centrifugal unit (Amicon), which allowed for exchange of the imidazole-containing buffer with protein storage buffer (50 mM NaH_2PO_4, 300 mM NaCl, pH 8.0). Protein purification was assessed following separation of purified proteins (and their accompanying washes) on a 12% SDS polyacrylamide gel and staining with Coomassie brilliant blue. Protein concentrations were determined using a Bradford assay (28), with bovine serum albumin as a standard.

Cell wall cleavage assays. An EnzChek lysozyme assay kit (Molecular Probes) was used to assess the ability of Rpfs to cleave fluorescein-labeled *Micrococcus lysodeikticus* (more commonly known as *M. luteus*) cell wall material *in vitro*. One nanomole of purified Rpf was added to each reaction mixture, and the volume was brought to 50 μl with 1× reaction buffer (100 mM sodium phosphate, 100 mM NaCl, pH 7.5) before the addition of 50 μl of the fluorescein-labeled*M. lysodeikticus* peptidoglycan substrate to each reaction mixture. One nanomole of the DNA-binding protein sIHF (29) was used as a negative control, while lysozyme (60 pmol, as per the manufacturer's recommendation) served as a positive control. Assays were performed in black 96-well plates (Thermo-Fisher). The amount of fluorescein released was measured every hour for 8 h using a Synergy 4 Microplate Reader (BioTek), with an excitation wavelength of 494 nm and an emission wavelength of 521 nm. Each assay was conducted using at least three independently isolated protein samples, with each protein activity assessed in triplicate.

Rpf interactions. To probe the potential for Rpf-Rpf protein interactions, the DNA corresponding to the mature Rpf sequences (lacking the signal peptide) were excised from their corresponding pET15b plasmid (Table 1) using NdeI and BamHI and cloned into both pGAD T7 activating domain (AD) and pGBK T7 binding domain (BD) vectors (Clontech) digested with the same enzymes. Conveniently, these vectors contain antibiotic selection markers to facilitate cloning in *E. coli* (ampicillin and kanamycin, respectively) and prototrophic markers for selection in yeast (Leu biosynthesis and Trp biosynthesis, respectively). pGAD T7 AD-Rpf and pGBK T7 BD-Rpf constructs were transformed into *S. cerevisiae* strains Y187 and Y2H Gold (Clontech), respectively, according to the TRAFO high-efficiency transformation protocol (30). Transformants were isolated on SD medium lacking Leu (Y187) or Trp (Y2H Gold) following incubation at 30°C for 3 days. To test for Rpf-Rpf interactions, single colonies (2 to 4 mm in diameter) of Rpf construct-containing Y2H Gold and Y187 strains were picked from 3-day-old plates and mixed together in 1 ml of 2× YPDA medium for mating. Cultures were incubated overnight at 30°C, after which cells were collected by centrifugation and plated on SD medium lacking both Trp and Leu. Single colonies were then patched onto SD plates lacking Trp and Leu to confirm the viability of the mated strains and on SD plates lacking Trp, Leu, adenine, and His to test for protein-protein interactions. Plates were examined for growth after 2 days of incubation at 30°C.

Gel filtration chromatography. Purified RpfB and a mutant variant lacking the three DUF348 domains (RpfBΔDUF348) were separated on a Superdex 75 column (GE Healthcare) preequilibriated with storage buffer (300 mM NaCl, 50 mM NaH_2PO_4, pH 8) to remove protein aggregates. Pure protein was applied to the column and eluted with storage buffer at a flow rate of 0.4 ml/min at 4°C. The absorbance of the eluate at 230 nm was recorded to confirm protein presence. Standards for column calibration (and assessment of protein oligomeric status) included RNase A (13.7 kDa), chymotrypsinogen A (25 kDa), ovalbumin (43 kDa), and albumin (67 kDa). Peak fractions were pooled and separated on a 12% SDS polyacrylamide gel stained with Coomassie brilliant blue to confirm the presence of RpfB/RpfBΔDUF348.

RESULTS

Bioinformatic analysis of the Rpfs in *S. coelicolor*. *S. coelicolor* encodes at least 60 proteins having domains with predicted peptidoglycan cleavage capabilities, and of these, seven possess an Rpf-like domain (20, 25). Of these seven, two (SCO2326 and SCO5029) appeared to be more distantly related to the well-characterized Rpf domains from *Micrococcus* and *Mycobacterium* (20) and lacked key catalytic residues (see Fig. S3 in the supplemental material); these were not considered further. The remaining five proteins (SCO0974, SCO3097, SCO3098, SCO3150, and SCO7458) bore domains that were highly similar to the crystallized *M. tuberculosis* RpfB protein ($RpfB_{MTB}$) and contained both critical catalytic amino acids and important substrate binding residues (Fig. 1A). Of these five proteins, SCO3150 showed the greatest sequence divergence relative to $RpfB_{MTB}$ (Fig. 1A) but shared a similar domain architecture, with its Rpf domain positioned at the extreme C-terminal end of the protein, where it was preceded by a G5 domain having potential *N*-acetylglucosamine-binding activity (31) and three DUF348 domains whose functions are unknown (Fig. 1B). We have therefore designated this protein $RpfB_{SC}$. For all other *S. coelicolor* Rpf proteins, the Rpf domain was immediately adjacent to the signal peptide at the N-terminal end. SCO3097 (RpfA), SCO3098 (RpfC), and SCO0974 (RpfD) each also carried a downstream LysM peptidoglycan-binding domain, like the first characterized Rpf from *M. luteus* (Fig. 1B), while RpfD possessed an additional domain with predicted peptidase activity at its C-terminal end. SCO7458, or RpfE, in its mature form comprised solely an Rpf domain (Fig. 1B).

Within the streptomycetes, four of the five Rpf proteins were broadly conserved (RpfA, RpfB, RpfC, and RpfD), while the smallest protein, RpfE, was not encoded by any of the other well-characterized *Streptomyces* species (Table 2). Instead, *Streptomyces venezuelae* and *Streptomyces avermitilis* encoded additional LysM-containing Rpfs that lacked equivalent orthologues in *S. coelicolor* and *Streptomyces griseus* (Table 2).

Temporal expression of *rpf* genes during solid and liquid culture growth. As an initial characterization step, we monitored the transcription profiles of the five *rpf* genes to determine when these genes were expressed and whether their expression was coordinately regulated. RNA was harvested from plate-grown cultures during vegetative growth (24 h), aerial hyphae formation (48 h), and early and late sporulation (72 and 96 h). Transcript levels were then assessed using RT-qPCR. We could detect expression for only three of the *rpf* genes (*rpfA*, *rpfC*, and *rpfD*), with the levels of *rpfB* and *rpfE* being too low to obtain transcript profiles. For the detectable *rpf* genes, expression was highest during vegetative growth before levels dropped at the onset of aerial development (Fig. 2A).

Similar profiles were observed for *rpfA* and *rpfC* when transcripts extracted from liquid-grown cultures were examined. Note that *S. coelicolor* does not differentiate in liquid culture, and thus these profiles reflect expression in vegetatively growing cells

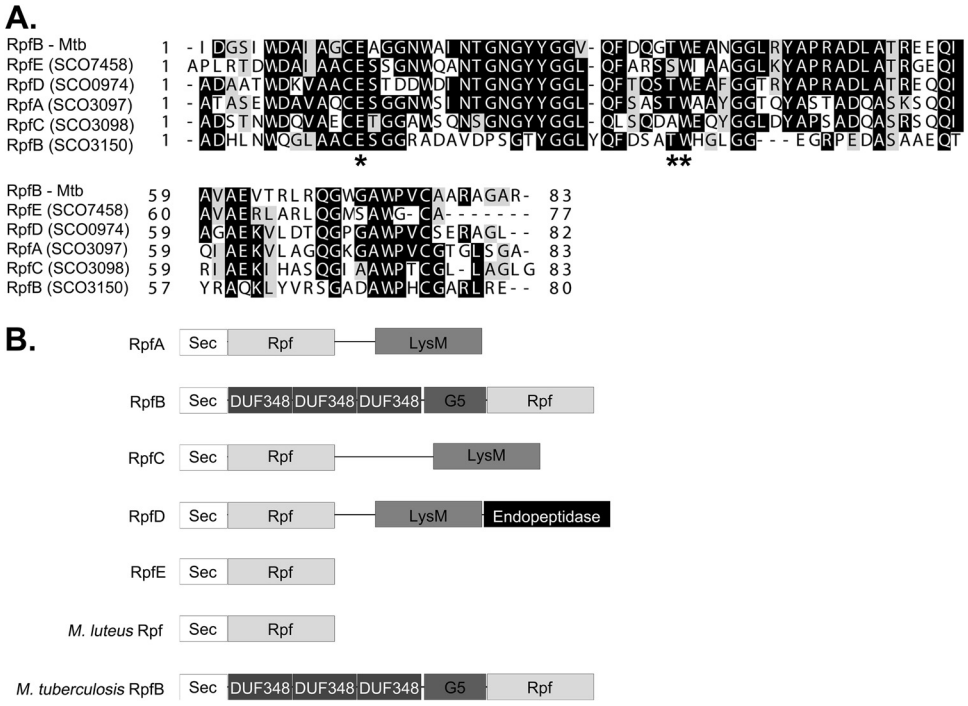

FIG 1 Sequence analysis of five Rpf homologues. (A) Multiple-sequence alignment of the Rpf domain from the five predicted Rpf proteins in *S. coelicolor*, together with RpfB from *Mycobacterium tuberculosis* ($RpfB_{MTB}$). Identical residues are highlighted in black. Similar residues are indicated in gray background. Key catalytic (Glu) and substrate-binding residues (Ser/Thr and Trp) are indicated with asterisks. (B) Schematic representation of the functional domain organization of the predicted Rpf proteins, along with *M. luteus* Rpf and $RpfB_{MTB}$. Sec, general secretion signal; Rpf, resuscitation-promoting factor domain; LysM, lysin motif; DUF348, domain of unknown function 348; G5, peptidoglycan-binding domain. Mtb, *M. tuberculosis*.

(Fig. 2A). A different pattern was detected for *rpfD*, however, where initial transcript levels were relatively low before rising during entry into stationary phase (~40 h) (Fig. 2A). As was the case for our solid culture samples, *rpfB* and *rpfE* transcripts were below the level of reliable detection.

Given the importance of *rpf* gene products in resuscitating dormant cells in *Mycobacterium* and *Micrococcus* (10, 11), we were interested in monitoring *rpf* transcription during spore germination. We were unable to do this using RT-qPCR (we could not isolate sufficient levels of RNA), so instead we constructed *rpf* promoter fusions to the *lux* reporter genes (32) and followed luminescence at 10-min intervals for the first 12 h of growth in liquid culture (spore germination was first seen at ~4 h under these growth conditions). We found that *rpfB* transcription began almost immediately and continued through the first 5 h of growth/germination (a similar expression pattern was occasionally seen for *rpfC* as well although it was not consistently observed), while *rpfA* expression was first detected at ~3 h, increased to maximal levels from ~5 to 6 h, and then dropped back to a low steady-state level (Fig. 2B). Expression from the other *rpf* promoters was below the detectable limit of the luminometer during this time course.

TABLE 2 Rpf domain-containing proteins in *S. coelicolor*, *S. avermitilis*, *S. venezuelae*, and *S. griseus*[a]

	Orthologue in[a]:		
S. coelicolor protein	*S. avermitilis*	*S. venezuelae*	*S. griseus*
RpfA (SCO3097)	SAV3534	SVEN2900	SGR4438
RrfB (SCO3150)	SAV3588	SVEN2970	SGR4355
RpfC (SCO3098)	SAV3535	SVEN2901	SGR4437
RpfD (SCO0974)	SAV7250	SVEN6803	SGR745
RpfE (SCO7458)			

[a] Although the other species did not encode RpfE, additional LysM-containing Rpfs were present in *S. avermitilis* (SAV6528 and SAV6527) and *S. venezuelae* (SVEN1384) that lacked orthologues in *S. coelicolor* and *S. griseus*.

Rpfs are important for initiating germination. Given the early transcription of *rpfA* and *rpfB* (and sometimes *rpfC*) and the resuscitation-associated function of the Rpfs as a whole, we sought to determine whether the Rpfs played a role in spore germination, i.e., the "dormant cell resuscitation" equivalent in *Streptomyces*. We first constructed strains bearing individual *rpf* deletions (*rpfA*, *rpfB*, *rpfC*, and *rpfE*) or disruptions (*rpfD*). As peptidoglycan lytic enzymes are notoriously redundant in their activities (33), we also generated strains with deletions in increasing numbers of *rpf* genes (deletions of two, three, four, and five *rpf* genes) with the goal of gaining a clearer picture as to the role of Rpf domain-containing proteins in *S. coelicolor* germination, growth, and development.

Spore germination for single and multiple *rpf* mutant strains was monitored over a 12-h time course, with spores being scored for the presence of one or more germ tubes using light microscopy (Fig. 3A). We found that, generally, loss of individual *rpf* genes was correlated with a delay in the onset of germination. The most significant delays were observed for *rpfA* and *rpfE* single mutants, and subtle but reproducible germination delays were seen for the *rpfD* mutant; loss of *rpfB* had no effect on spore germination, whereas *rpfC* mutants occasionally took longer than the wild type

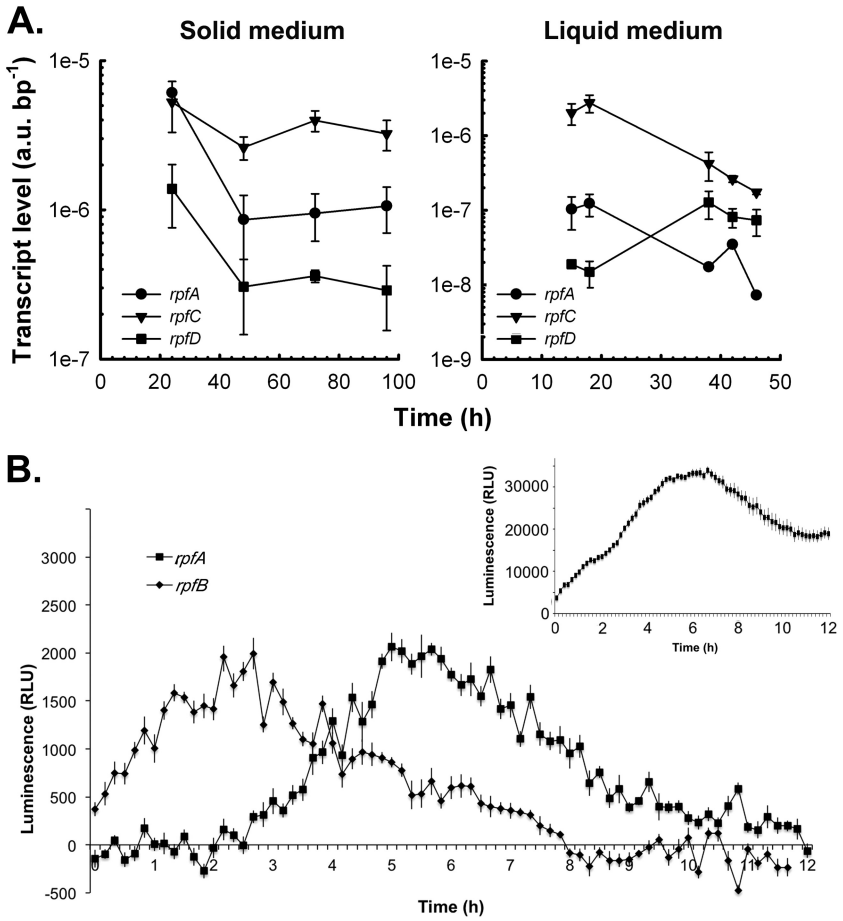

FIG 2 Transcript levels of Rpf-encoding genes in *S. coelicolor* throughout growth and development. (A) The *S. coelicolor* wild-type strain M145 was grown at 30°C on MS agar medium and TSB-YEME liquid medium. At the times indicated, total RNA was extracted from cells, and transcripts bearing the *rpfA*, *rpfC*, and *rpfD* coding regions were quantified using RT-qPCRs. Transcript levels were normalized to total RNA mass and PCR product length. The quantification cycle value of each no-RT control was greater than that of the +RT samples by at least 10 cycles. Quantification cycle values of all no-template controls were consistently greater than 40 cycles. All data are presented as means ± standard errors ($n = 1$ to 3). au, arbitrary units. (B) *rpf* promoter activities were monitored in TSB-YEME liquid medium for 12 h postinoculation using a luminescence-based reporter. The inset panel (positive control) represents the activity of the strong constitutive *ermE** promoter fused to the *lux* genes over the same 12-h time course. Data are presented as means ± standard errors ($n = 8$). RLU, relative light units.

to initiate germination. Somewhat surprisingly, we found that the initial delay in germination did not translate into a longer time frame needed for complete germination to occur: all spores (mutant and wild type) were fully germinated by 12 h. The germination defect for the *rpfA* mutant has been complemented previously (25), and here we were able to partially complement the defect observed for the *rpfD* and *rpfE* mutants with a wild-type copy of their respective genes (see Fig. S4 in the supplemental material).

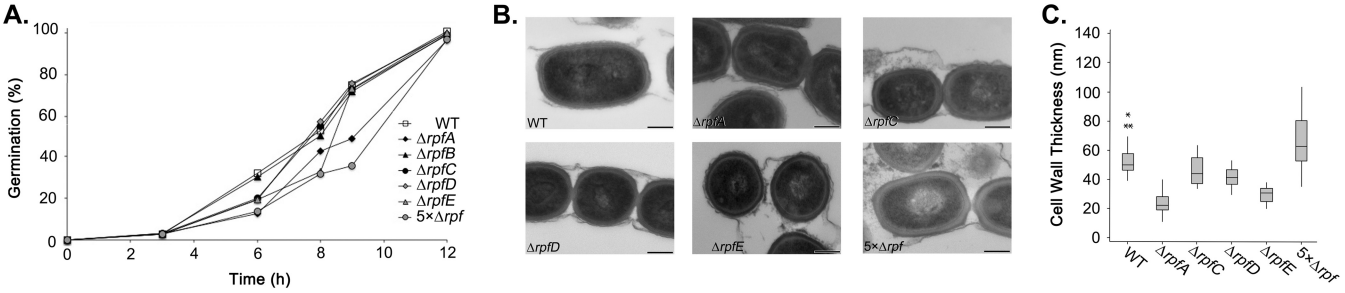

FIG 3 Rpfs are involved in initiating germination of *S. coelicolor* spores. (A) Wild-type (WT), individual *rpf* mutants, and 5× Δ*rpf* mutant spores were monitored for germination using light microscopy over 12 h. The proportion of germinated spores was determined for each strain at the indicated time points. Data are representative of three independent trials ($n > 100$ spores for every time point, for every strain). (B) Transmission electron micrographs of wild-type, individual *rpf* mutants, and 5× Δ*rpf* mutant strains. Scale bar, 250 nm. (C) Wall widths of spores ($n > 25$) from the samples shown in panel B were determined from transmission electron micrographs. Box plots indicate the median (center band), the 25th and 75th percentiles (lower and upper limits of the box, respectively), and the 5th and 95th percentiles (lower and upper whiskers, respectively). Asterisks indicate outliers.

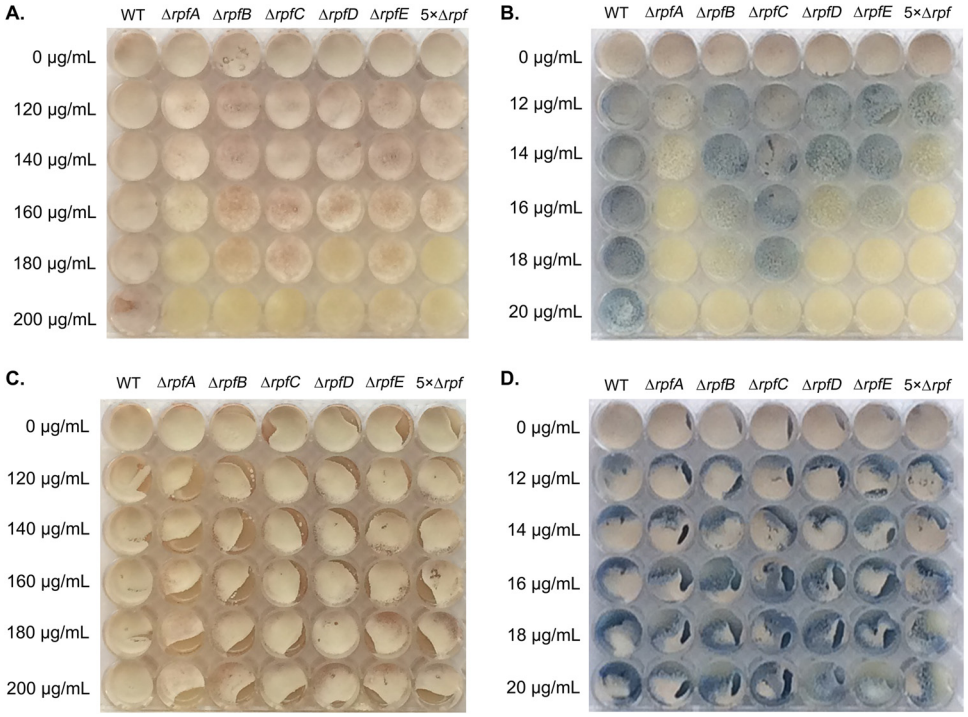

FIG 4 Rpf deletion enhances antibiotic sensitivity during germination. Equal numbers of mutant and wild-type (WT) spores were spread on MS agar containing the indicated amounts of D-cycloserine (A) or bacitracin (B) or were inoculated onto MS agar and allowed to germinate for 16 h before being overlaid with the indicated amounts of D-cycloserine (C) or bacitracin (D). Plates were incubated for 4 days at 30°C. Images are representative of three independent replicates.

Of the multiple *rpf* mutant strains, the strain with deletions of *rpfA* through *rpfE* (5× Δ*rpf* mutant) showed the greatest impairment in germination: germ tubes had emerged from fewer than 40% of spores after 9 h although, as was seen for the single mutants, germination was complete by 12 h (Fig. 3A; data not shown). Collectively, the delay in initiating germination seen for the *rpf* mutants indicates that these proteins play an important (although not essential) role in promoting spore germination.

Delayed germination in these strains could stem directly from the lack of Rpfs, which may be needed to remodel the spore peptidoglycan during germination and/or release a germination-promoting signal. Alternatively, the germination defects could stem from Rpf-dependent changes in spore peptidoglycan architecture such that the spore wall is less amenable to germ tube emergence. Indeed, deleting peptidoglycan hydrolases has been associated with increased cell wall thickness in *Bacillus subtilis* (34, 35). To determine whether this was a possibility, we probed spore wall thickness for those *rpf* mutants exhibiting germination delays and found that there was no correlation between spore wall thickness and germination rate. Of the single mutants, the *rpfA* strain exhibited the greatest germination defect, yet *rpfA* mutant spores had the thinnest walls of all strains tested (25) (Fig. 3B and C). In contrast, the spore walls of the 5× mutant were at least as thick as those of the wild type, and this mutant showed the greatest delay of all strains (Fig. 3B and C). While these experiments do not preclude the possibility that altered cell wall structure contributes to delayed germination, they do indicate that wall thickness alone cannot be used as a surrogate for germination competence.

Germinating spores lacking Rpfs are more sensitive to cell wall-specific antibiotics. To determine whether the germination defects and heterogeneous spore wall thickness of the different *rpf* mutants might reflect altered cell wall properties, we tested the different mutants for their sensitivity to antibiotics targeting the cell wall. Mutant and wild-type spores were plated on MS agar containing increasing amounts of D-cycloserine (inhibitor of D-Ala–D-Ala ligase) (Fig. 4A) and bacitracin (inhibitor of C_{55}-bactoprenol pyrophosphate dephosphorylation) (Fig. 4B). As a control, we also tested all strains for their sensitivity to hygromycin, an antibiotic targeting protein synthesis. Relative to the wild type, all *rpf* mutants showed increased sensitivity to D-cycloserine and bacitracin, with the Δ*rpfA*, Δ*rpfD*, and the 5× Δ*rpf* strains being the most sensitive; all strains (wild type and mutant) were equally sensitive to hygromycin (data not shown). To determine if the increased *rpf* mutant sensitivity reflected a germination-specific defect, mutant and wild-type spores were spread on MS agar and grown for 16 h to allow for complete germination. The vegetatively growing cells were then overlaid with increasing amounts of D-cycloserine (Fig. 4C) or bacitracin (Fig. 4D). In contrast to our previous results, the *rpf* mutant strains were resistant to all concentrations of both antibiotics. This suggested that Rpf activity alters the spore wall—or that of the initial germ tubes—such that Rpf-deficient strains display enhanced sensitivity to antibiotics that block cell wall synthesis.

Deleting *rpf* genes impacts vegetative growth in liquid culture. To further probe the biological role of the Rpf proteins in *S. coelicolor*, we followed the growth and development of the individual and multiple *rpf* mutant strains on solid agar plates (sporulation-specific [MS] and rich [R5] media). After 2 days, the majority of *rpf* mutants appeared largely wild type (Fig. 5A) and remained so after additional incubation (data not shown).

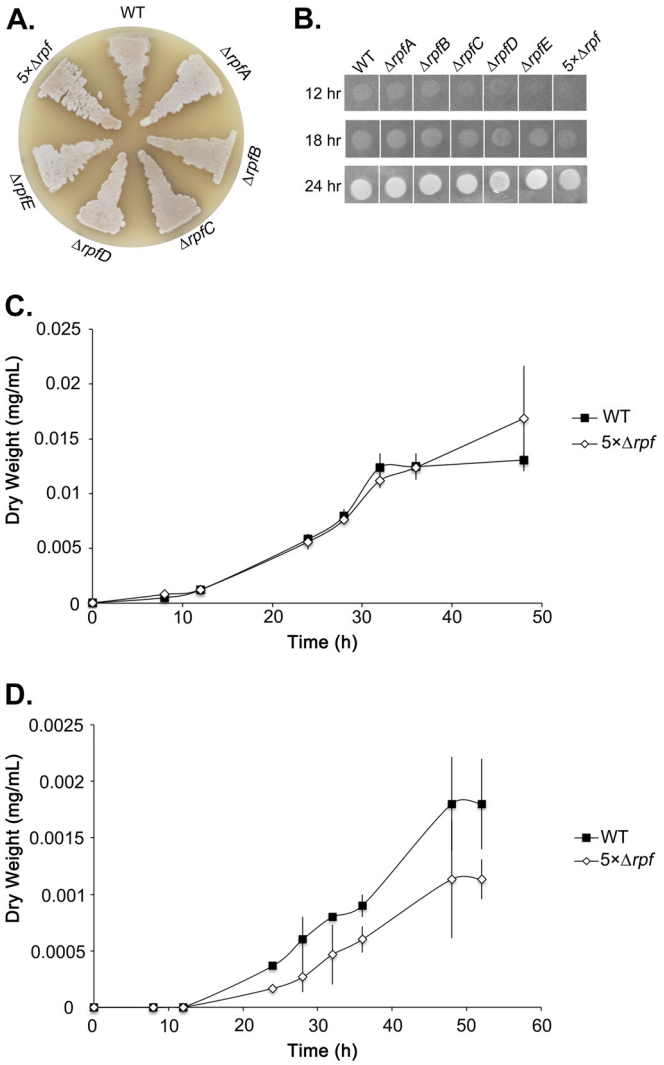

FIG 5 Phenotypic analyses of *rpf* mutant strains. (A) Colony morphology of the wild type, individual *rpf* mutants, and 5× Δ*rpf* deletion strains after 2 days growth on MS agar medium. (B) A total of 2×10^5 mutant and wild-type spores were plated on LB agar medium (a low-Mg^{2+} medium used to exacerbate any cell wall defects). Pictures were taken at the indicated time points and are representative of three independent trials. (C and D) Growth profile of the 5× Δ*rpf* mutant compared to the wild type during liquid culture in TSB-YEME medium (C) and NMMP medium (D). Values are presented as means ± standard errors ($n = 3$). WT, wild type.

For the *rpf* genes whose expression was detectable, transcript levels were generally highest during germination and vegetative growth, with the exception of the level of *rpfD* in liquid culture. To determine whether any of the *rpf* mutations had an effect on vegetative growth, we followed colony growth over a 24-h time course on solid medium (Fig. 5B). We did not observe any delays in the growth of the *rpfA* or *rpfB* mutant, but the growth of *rpfC*, *rpfD*, and *rpfE* mutants was slightly retarded at 12 h. Intriguingly, the 5× Δ*rpf* mutant failed to form a detectable colony after 12 h, and its growth was detectable only by 18 h (Fig. 5C). It is conceivable that these growth delays simply reflected slower germination rates; however, this cannot be the only explanation as the *rpfC* strain had largely normal germination but showed delayed vegetative growth, while the *rpfA* mutant had a significant germination delay but exhibited robust vegetative growth.

As defects in vegetative growth may be more pronounced in liquid culture, we followed the growth profile of the 5× Δ*rpf* mutant relative to its wild-type parent strain in rich and minimal media. In rich medium, the growth curve of the 5× Δ*rpf* mutant was virtually indistinguishable from that of the wild-type strain prior to stationary phase, at which point the 5× Δ*rpf* mutant showed better growth than the wild type (Fig. 5D). In contrast, in minimal medium, the 5× Δ*rpf* mutant grew far less robustly than the wild type at all time points, suggesting that the Rpfs confer a distinct competitive advantage during growth under nutrient-limiting conditions.

***In vitro* activity assays of each Rpf protein reveal widely various levels of peptidoglycan cleavage capabilities.** To begin probing the biochemical basis for Rpf function, we set out to assess the ability of each of these enzymes to cleave purified peptidoglycan. As a substrate, we opted to use commercially available and fluorescently labeled peptidoglycan from the close *Streptomyces* relative *M. luteus*. The fluorescein labeling density was sufficiently high that fluorescence was quenched; this quenching could be alleviated through cleavage of the labeled peptidoglycan, with increased fluorescence being directly proportional to cleavage activity. We overexpressed and purified each of the five Rpf enzymes and monitored their activity over 8 h. While all Rpfs were significantly less active than lysozyme (positive control), there were considerable differences in their activity levels. RpfE was the most active enzyme, followed by RpfA and RpfD. RpfB and RpfC had the lowest activities, with their levels always being less than half that of any other enzyme (Fig. 6). sIHF, a cytoplasmic DNA-binding protein from *S. coelicolor*, was also overexpressed, purified, and subjected to the cleavage assay to ensure that any activity observed was not due to contaminating *E. coli* proteins. These results indicate that all of the *S. coelicolor* Rpfs have some level of peptidoglycan cleavage capability and thus would be able to remodel *Streptomyces* cell walls.

Rpf interactions: RpfB forms a dimer. Previous work in *Mycobacterium* has suggested that several Rpfs interact with other cell wall-lytic enzymes (17). In particular, the RipA endopeptidase interacts with $RpfB_{MTB}$, and this association results in synergistic activity. RipA further interacts with $RpfE_{MTB}$, an enzyme like RpfE in *S. coelicolor* that lacks an obvious means of associating with the peptidoglycan (17, 18). There is no RipA homologue encoded by the streptomycetes, and thus we wondered whether RpfD, with its endopeptidase domain, might interact with RpfB and whether any of the LysM domain-containing Rpfs (RpfA, RpfB, or RpfD) might associate with RpfE, helping to anchor it to the cell wall. To test this hypothesis we examined interactions between each Rpf protein (excluding their signal peptides) using a yeast two-hybrid system. Rpf interactions were tested in a pairwise fashion, with each mating pair spread on diagnostic medium such that only the strains with an interacting Rpf pair would be capable of growing. We found that RpfB associated with itself, based on the robust growth observed for this mating pair on selective medium, in contrast to all other Rpf pairs, which were unable to interact in this system (Fig. 7A).

To further test the oligomerization capabilities of RpfB, we overexpressed and purified mature RpfB and followed its oligomeric status using gel filtration chromatography. We found that RpfB eluted at a volume that was most consistent with a dimer form (molecular mass of the His-tagged fusion protein was 36.6

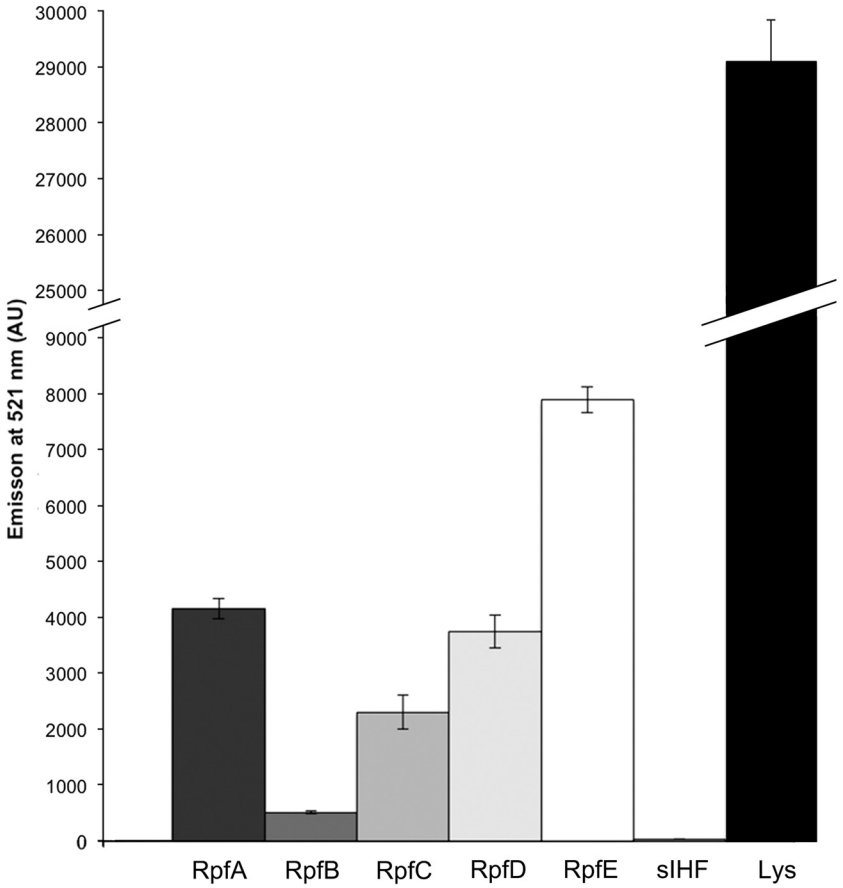

FIG 6 Rpf proteins cleave peptidoglycan *in vitro*. One nanomole of pure protein (as indicated) was mixed with fluorescein-labeled *M. luteus* cell walls. Data represent the average emission at 521 nm after 8 h of incubation of three trials ± 1 standard error. Negative control, cytoplasmic DNA binding protein sIHF; positive control, lysozyme (Lys). AU, arbitrary units.

kDa), with no detectable monomer species observed (Fig. 7B), supporting our yeast two-hybrid observations.

Removal of the DUF348 domains from RpfB impacts dimerization and enhances enzyme activity. RpfB does not possess any obvious protein interaction domains (Fig. 1B): its G5 domain is predicted to promote peptidoglycan binding (31), while the Rpf domain failed to promote dimerization in any of the other Rpf protein combinations tested here. DUF348 domains are

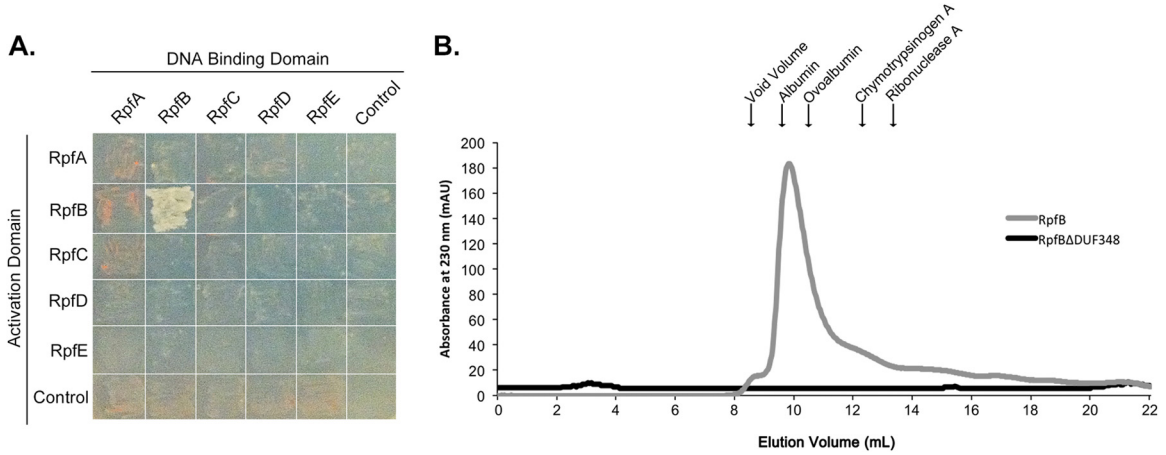

FIG 7 RpfB forms dimers. (A) Yeast two-hybrid analysis of interactions between Rpf proteins. Pictures were taken after 2 days of incubation at 30°C. Growth on selective medium indicates an interaction between bait (DNA-binding domain)- and prey (activation domain)-associated proteins. (B) Purified RpfB and RpfBΔDUF348 were separated on a Sephadex 75 gel filtration column. The peak at 9.4 ml represents likely RpfB dimers. RpfBΔDUF348 dimers were expected to elute at 12 ml. The molecular mass and elution volume, respectively, of each of the standards indicated above the figure are as follows: albumin, 67 kDa and 9.6 ml; ovalbumin, 43 kDa and 10.4 ml; chymotrypsinogen A, 25 kDa and 12.4 ml; and RNase A, 13.7 kDa and 13.3 ml.

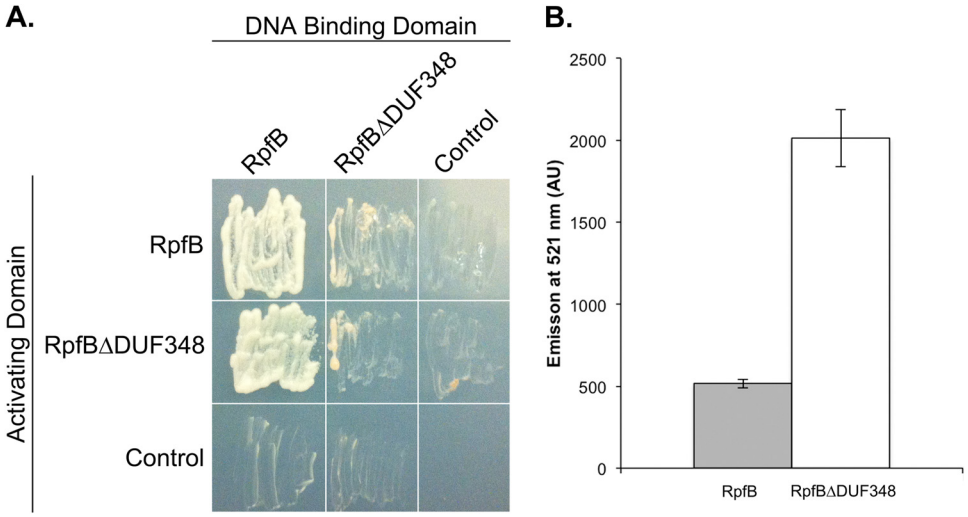

FIG 8 The DUF348 domains in RpfB are required for dimerization and inhibit RpfB activity. (A) Yeast two-hybrid analysis of interactions between full-length and truncated RpfB proteins, as described in the legend to Fig. 6. Pictures were taken after 2 days of incubation at 30°C on selective medium. The level of growth is correlated with the strength of the protein interaction. (B) One nanomole of pure protein was incubated with fluorescein-labeled *M. luteus* cell wall for 8 h. Fluorescence emitted at 521 nm was quantified. Data are presented as means ± standard errors ($n = 3$).

frequently associated with proteins functioning at the cell wall (20, 36), but, as their name implies, their function is unknown; these domains therefore seemed the most likely candidates for mediating dimerization. To test the role of the DUF348 sequences in RpfB dimerization, we constructed a truncated version of RpfB in which the three DUF348 domains were removed (RpfBΔDUF348). We found that RpfBΔDUF348 failed to interact as robustly with itself as it did with the full-length mature RpfB protein, and its ability to interact with RpfB differed, depending on the vector system (Fig. 8A). To further probe the role of DUF348 domains in dimerization, we again conducted gel filtration chromatography. While RpfB appeared to elute predominantly as a dimer, no dimers were observed for RpfBΔDUF348 (molecular mass of the His-tagged fusion was 21.5 kDa) (Fig. 7B). Instead, it did not elute as a discrete peak at all and appeared to interact with the column, eluting only after 24 ml (data not shown), suggesting that it had a very different conformation than full-length RpfB.

Given this observation, we sought to determine whether the DUF348 domains influenced RpfB activity. We tested the peptidoglycan cleavage activity of RpfBΔDUF348 in our fluorescent substrate assay and found its activity to be far greater than that of the full-length RpfB, suggesting that these domains may function to modulate enzyme activity (Fig. 8B).

DISCUSSION

Rpfs and their role in resuscitation. Rpf enzymes were originally defined on the basis of their resuscitation-promoting activities in *Micrococcus* and, later, in *Mycobacterium*. Our results support a role for the Rpfs in spore germination in *S. coelicolor*; however, they do not all contribute equivalently, and the fact that germination can proceed (albeit without wild-type kinetics) in the complete absence of Rpfs suggests that they must function in conjunction with other factors. Of the individual Rpfs, *rpfA* mutants had the most severe germination defect, with *rpfB* and *rpfC* mutants behaving most like the wild type. For the *rpfB* mutant, this could be explained in part by the fact that RpfB reproducibly exhibited the lowest *in vitro* cleavage activity of all the Rpfs. In contrast, *rpfC* was not routinely transcribed during germination, and we expected that it may have little to no enzymatic activity because, unlike the other Rpfs, it lacks a key substrate binding residue, having an Ala in place of a Ser/Thr residue (19) (Fig. 1A). Surprisingly, we found it to have intermediate levels of activity, suggesting that this residue is not critical for substrate recognition and binding. In examining the sequence of the RpfC orthologues in other streptomycetes, this particular residue varied considerably, with everything from Leu (*Streptomyces* sp. strain S4) and Asn (*S. avermitilis* and *Streptomyces scabies*) through to the expected Ser (*S. venezuelae*) and Thr (*S. griseus* and *Streptomyces clavuligerus*) residues found at this position (see Fig. S5 in the supplemental material).

The germination defect observed for the *rpfE* mutant was surprising, given that *rpfE* transcripts were undetectable. It is possible that low levels of expression are all that are required for its function; this would be consistent with previous observations in *M. luteus*, where the lone Rpf could restore active growth at extremely low (picomolar) concentrations (10).

The 5× Δ*rpf* mutant exhibited the most severe defect in germination and subsequent vegetative outgrowth. These defects did not dramatically impact the growth of this strain under nutrient-rich conditions; however, in minimal medium, growth of this strain was severely attenuated compared with that of the wild type. This suggests that for *Streptomyces* species growing in a nutrient-poor soil environment, the lack of Rpf enzymes may confer a profound fitness cost, analogous to that seen for other bacteria (37).

Rpf redundancy in the *Streptomycetes*. Within the *Actinobacteria*, *M. luteus* encodes a single Rpf enzyme that is essential for viability. In contrast, *Streptomyces* and *Mycobacterium* species encode four or more Rpf domain-containing enzymes, and at least in a laboratory environment, these Rpf-encoding genes can all be deleted without compromising viability. In *M. tuberculosis*, studies have suggested that deleting $rpfB_{MTB}$ (homologous to *rpfB* in *S. coelicolor*) delays *M. tuberculosis* resuscitation in a chronic tuber-

culosis model (14) although single deletions of any other *rpf* gene had no obvious effect. Combining mutations led to more severe phenotypic consequences, with double and triple *rpf* mutants attenuated in their ability both to resuscitate dormant cells *in vitro* and to establish chronic infections *in vivo* (16, 38, 39).

In *S. coelicolor*, we found that individual *rpf* deletions conferred modest germination defects, with differing levels of severity. This suggested that these enzymes make distinct contributions to germination and vegetative outgrowth, a possibility supported by the fact that individual Rpfs possessed distinct functional domains, and were expressed at various levels and, in some cases, at different times. We did not, however, observe directly additive phenotypic effects when multiple *rpf* genes were deleted, suggesting that there is some level of functional redundancy shared by these enzymes. Notably, in strains lacking all Rpfs, spore germination was still complete by 12 h, despite the marked delay in germination initiation. This suggests that the resuscitation process in *Streptomyces* is more complex than that in either *Mycobacterium* or *Micrococcus* and that the Rpfs may function as part of a larger peptidoglycan-remodeling network.

Rpf interactions. In considering the Rpf proteins encoded by *Streptomyces* and *Mycobacterium*, only RpfB shared full-length similarity. Previous work in *Mycobacterium* had shown that while the *rpfB* mutation had phenotypic consequences, *in vitro* assays revealed RpfB to have little activity on its own (19), a phenomenon we also observed in our *in vitro* assays here. Subsequent investigations revealed a key interaction between RpfB and the endopeptidase RipA and synergistic peptidoglycan cleavage by the two enzymes (17, 18).

The dimerization capability of RpfB had not been previously recognized as the screen that led to RipA identification included only the Rpf domain of RpfB (17), and the Rpf domain does not appear to promote dimerization, based on the lack of interaction seen for all other Rpfs. Our results suggest that, instead, the DUF348 domains found at the N terminus of RpfB facilitate dimerization and inhibit RpfB enzyme activity. It is tantalizing to speculate that the RipA-RpfB association in *Mycobacterium* may lead to a conformational change in RpfB, alleviating the DUF348-mediated inhibition of enzyme activity. DUF348 domains are found in proteins throughout the *Actinobacteria* and *Firmicutes* and in most cases are found together with both G5 and peptidoglycan cleavage-associated domains (in *S. coelicolor*, these domains are not present in any protein but RpfB). Our results indicate that DUF348 domains may serve as a means of controlling the activity of peptidoglycan-cleaving enzymes.

Given the potentially destructive nature of cell wall-lytic enzymes like the Rpfs, it is critically important that their activity be tightly controlled. Increasingly, protein-protein interactions are being found to contribute to this regulation. In *M. tuberculosis*, RpfB-RipA activity is negatively influenced by interactions with penicillin binding protein 1 (PBP1) (40), while in *E. coli*, two amidases responsible for cell separation are controlled by peptidoglycan-binding enzymes that confer spatial and temporal regulation (41). Notably, the two regulatory proteins in *E. coli* were initially classified as having peptidoglycan cleavage activity themselves, specifically, endopeptidase activity. It will be interesting to see whether equivalent proteins control any of the Rpf enzymes in *S. coelicolor*.

ACKNOWLEDGMENTS

We thank Tamiza Nanji and Alba Guarné for their assistance with the gel filtration chromatography experiments and Matt Moody and Rachel Young for their assistance with figure construction.

This work was supported by a Vanier Canada Graduate Scholarship to R.J.S.-O., by an Ontario Graduate Scholarship to H.J.H., by the Canada Research Chairs program (to M.A.E.), by a grant from the Canadian Institutes for Health Research (to M.A.E.; grant no. MOP-93635), and by the Natural Sciences and Engineering Research Council of Canada (to M.A.E.; Discovery grant no. 312495).

REFERENCES

1. **Hopwood DA.** 2007. *Streptomyces* in nature and medicine: the antibiotic makers Oxford University Press New York, NY.
2. **Flärdh K, Buttner MJ.** 2009. *Streptomyces* morphogenetics: dissecting differentiation in a filamentous bacterium. Nat Rev Microbiol **7:**36–49. http://dx.doi.org/10.1038/nrmicro1968.
3. **Flärdh K, Richards DM, Hempel AM, Howard M, Buttner MJ.** 2012. Regulation of apical growth and hyphal branching in *Streptomyces*. Curr Opin Microbiol **15:**737–743. http://dx.doi.org/10.1016/j.mib.2012.10.012.
4. **Elliot MA, Flärdh K.** 2012. *Streptomyces* spores, encyclopedia of life sciences. John Wiley & Sons, Ltd., Chichester, United Kingdom.
5. **Rittershaus ES, Baek SH, Sassetti CM.** 2013. The normalcy of dormancy: common themes in microbial quiescence. Cell Host Microbe **13:**643–651. http://dx.doi.org/10.1016/j.chom.2013.05.012.
6. **Kim JH, O'Brien KM, Sharma R, Boshoff HI, Rehren G, Chakraborty S, Wallach JB, Monteleone M, Wilson DJ, Aldrich CC, Barry CE, III, Rhee KY, Ehrt S, Schnappinger D.** 2013. A genetic strategy to identify targets for the development of drugs that prevent bacterial persistence. Proc Natl Acad Sci U S A **110:**19095–19100. http://dx.doi.org/10.1073/pnas.1315860110.
7. **Meador-Parton J, Popham DL.** 2000. Structural Analysis of *Bacillus subtilis* spore peptidoglycan during sporulation. J Bacteriol **182:**4491–4499. http://dx.doi.org/10.1128/JB.182.16.4491-4499.2000.
8. **Seiler P, Ulrichs T, Bandermann S, Pradl L, Jorg S, Krenn V, Morawietz L, Kaufmann SH, Aichele P.** 2003. Cell-wall alterations as an attribute of *Mycobacterium tuberculosis* in latent infection. J Infect Dis **188:**1326–1331. http://dx.doi.org/10.1086/378563.
9. **Keep NH, Ward JM, Robertson G, Cohen-Gonsaud M, Henderson B.** 2006. Bacterial resuscitation factors: revival of viable but non-culturable bacteria. Cell Mol Life Sci **63:**2555–2559. http://dx.doi.org/10.1007/s00018-006-6188-2.
10. **Mukamolova GV, Kaprelyants AS, Young DI, Young M, Kell DB.** 1998. A bacterial cytokine. Proc Natl Acad Sci U S A **95:**8916–8921. http://dx.doi.org/10.1073/pnas.95.15.8916.
11. **Mukamolova GV, Turapov OA, Kazarlan K, Telkov M, Kaprelyants AS, Kell DB, Young M.** 2002. The *rpf* gene of *Micrococcus luteus* encodes an essential secreted growth factor. Mol Microbiol **46:**611–621. http://dx.doi.org/10.1046/j.1365-2958.2002.03183.x.
12. **Mukamolova GV, Turapov OA, Young DI, Kaprelyants AS, Kell DB, Young M.** 2002. A family of autocrine growth factors in *Mycobacterium tuberculosis*. Mol Microbiol **46:**623–635. http://dx.doi.org/10.1046/j.1365-2958.2002.03184.x.
13. **Tufariello JM, Jacobs WR, Chan J.** 2004. Individual *Mycobacterium tuberculosis* resuscitation-promoting factor homologues are dispensable for growth *in vitro* and *in vivo*. Infect Immun **72:**515–526. http://dx.doi.org/10.1128/IAI.72.1.515-526.2004.
14. **Tufariello JM, Mi K, Xu J, Manabe YC, Kesavan AK, Drumm J, Tanaka K, Jacobs WR, Jr, Chan J.** 2006. Deletion of the *Mycobacterium tuberculosis* resuscitation-promoting factor *Rv1009* gene results in delayed reactivation from chronic tuberculosis. Infect Immun **74:**2985–2995. http://dx.doi.org/10.1128/IAI.74.5.2985-2995.2006.
15. **Kana BD, Gordhan BG, Downing KJ, Sung N, Vostroktunova G, Machowski EE, Tsenova L, Young M, Kaprelyants A, Kaplan G, Mizrahi V.** 2008. The resuscitation-promoting factors of *Mycobacterium tuberculosis* are required for virulence and resuscitation from dormancy but are collectively dispensable for growth *in vitro*. Mol Microbiol **67:**672–684. http://dx.doi.org/10.1111/j.1365-2958.2007.06078.x.
16. **Russell-Goldman E, Xu J, Wang X, Chan J, Tufariello JM.** 2008. A *Mycobacterium tuberculosis* Rpf double-knockout strain exhibits profound defects in reactivation from chronic tuberculosis and innate immu-

nity phenotypes. Infect Immun **76:**4269–4281. http://dx.doi.org/10.1128/IAI.01735-07.
17. **Hett EC, Chao MC, Steyn AJ, Fortune SM, Deng LL, Rubin EJ.** 2007. A partner for the resuscitation-promoting factors of *Mycobacterium tuberculosis*. Mol Microbiol **66:**658–668. http://dx.doi.org/10.1111/j.1365-2958.2007.05945.x.
18. **Hett EC, Chao MC, Deng LL, Rubin EJ.** 2008. A mycobacterial enzyme essential for cell division synergizes with resuscitation-promoting factor. PLoS Pathog **4:**e1000001. http://dx.doi.org/10.1371/journal.ppat.1000001.
19. **Cohen-Gonsaud M, Barthe P, Bagneris C, Henderson B, Ward J, Roumestand C, Keep NH.** 2005. The structure of a resuscitation-promoting factor domain from *Mycobacterium tuberculosis* shows homology to lysozymes. Nat Struct Mol Biol **12:**270–273. http://dx.doi.org/10.1038/nsmb905.
20. **Ravagnani A, Finan CL, Young M.** 2005. A novel firmicute protein family related to the actinobacterial resuscitation-promoting factors by non-orthologous domain displacement. BMC Genomics **6:**39. http://dx.doi.org/10.1186/1471-2164-6-39.
21. **Kieser T, Bibb MJ, Buttner MJ, Chater KF, Hopwood DA.** 2000. Practical *Streptomyces* genetics. John Innes Foundation, Norwich, United Kingdom.
22. **Moody MJ, Young RA, Jones SE, Elliot MA.** 2013. Comparative analysis of non-coding RNAs in the antibiotic-producing *Streptomyces* bacteria. BMC Genomics **14:**558. http://dx.doi.org/10.1186/1471-2164-14-558.
23. **Peirson SN, Butler JN, Foster RG.** 2003. Experimental validation of novel and conventional approaches to quantitative real-time PCR data analysis. Nucleic Acids Res **31:**e73. http://dx.doi.org/10.1093/nar/gng073.
24. **Gust B, Challis GL, Fowler K, Kieser T, Chater KF.** 2003. PCR-targeted *Streptomyces* gene replacement identifies a protein domain needed for biosynthesis of the sesquiterpene soil odor geosmin. Proc Natl Acad Sci U S A **100:**1541–1546. http://dx.doi.org/10.1073/pnas.0337542100.
25. **Haiser HJ, Yousef MR, Elliot MA.** 2009. Cell wall hydrolases affect germination, vegetative growth, and sporulation in *Streptomyces coelicolor*. J Bacteriol **191:**6501–6512. http://dx.doi.org/10.1128/JB.00767-09.
26. **Schneider CA, Rasband WS, Eliceiri KW.** 2012. NIH Image to ImageJ: 25 years of image analysis. Nat Methods **9:**671–675. http://dx.doi.org/10.1038/nmeth.2089.
27. **Petersen TN, Brunak S, von Heijne G, Nielsen H.** 2011. SignalP 4.0: discriminating signal peptides from transmembrane regions. Nat Methods **8:**785–786. http://dx.doi.org/10.1038/nmeth.1701.
28. **Bradford MM.** 1976. A rapid and sensitive method for the quantitation of microgram quantities of protein utilizing the principle of protein-dye binding. Anal Biochem **72:**248–254. http://dx.doi.org/10.1016/0003-2697(76)90527-3.
29. **Swiercz JP, Nanji T, Gloyd M, Guarne A, Elliot MA.** 2013. A novel nucleoid-associated protein specific to the actinobacteria. Nucleic Acids Res **41:**4171–4184. http://dx.doi.org/10.1093/nar/gkt095.
30. **Gietz RD, Schiestl RH.** 2007. High-efficiency yeast transformation using the LiAc/SS carrier DNA/PEG method. Nat Protoc **2:**31–34. http://dx.doi.org/10.1038/nprot.2007.13.
31. **Bateman A, Holden MT, Yeats C.** 2005. The G5 domain: a potential *N*-acetylglucosamine recognition domain involved in biofilm formation. Bioinformatics **21:**1301–1303. http://dx.doi.org/10.1093/bioinformatics/bti206.
32. **Craney A, Hohenauer T, Xu Y, Navani NK, Li Y, Nodwell J.** 2007. A synthetic *luxCDABE* gene cluster optimized for expression in high-GC bacteria. Nucleic Acids Res **35:**e46. http://dx.doi.org/10.1093/nar/gkm086.
33. **Typas A, Banzhaf M, Gross CA, Vollmer W.** 2012. From the regulation of peptidoglycan synthesis to bacterial growth and morphology. Nat Rev Microbiol **10:**123–136. http://dx.doi.org/10.1038/nrmicro2677.
34. **Fan DP, Beckman MM.** 1971. Mutant of *Bacillus subtilis* demonstrating the requirement of lysis for growth. J Bacteriol **105:**629–636.
35. **Fan DP, Pelvit MC, Cunningham WP.** 1972. Structural difference between walls from ends and sides of the rod-shaped bacterium *Bacillus subtilis*. J Bacteriol **109:**1266–1272.
36. **Yeats CB, Bentley S, Bateman A.** 2003. New knowledge from old: *in silico* discovery of novel protein domains in *Streptomyces coelicolor*. BMC Microbiol **3:**3. http://dx.doi.org/10.1186/1471-2180-3-3.
37. **Segev E, Rosengerg A, Mamou G, Sinai L, Ben-Yehuda S.** 2013. Molecular kinetics of reviving bacterial spores. J Bacteriol **195:**1875–1882. http://dx.doi.org/10.1128/JB.00093-13.
38. **Downing KJ, Mischenko VV, Shleeva MO, Young DI, Young M, Kaprelyants AS, Apt AS, Mizrahi V.** 2005. Mutants of *Mycobacterium tuberculosis* lacking three of the five *rpf*-like genes are defective for growth *in vivo* and for resuscitation *in vitro*. Infect Immun **73:**3038–3043. http://dx.doi.org/10.1128/IAI.73.5.3038-3043.2005.
39. **Biketov S, Potapov V, Ganina E, Downing K, Kana BD, Kaprelyants A.** 2007. The role of resuscitation promoting factors in pathogenesis and reactivation of *Mycobacterium tuberculosis* during intra-peritoneal infection in mice. BMC Infect Dis **7:**146. http://dx.doi.org/10.1186/1471-2334-7-146.
40. **Hett EC, Chao MC, Rubin EJ.** 2010. Interaction and modulation of two antagonistic cell wall enzymes of mycobacteria. PLoS Pathog **6:**e1001020. http://dx.doi.org/10.1371/journal.ppat.1001020.
41. **Uehara T, Bernhardt TG.** 2011. More than just lysins: peptidoglycan hydrolases tailor the cell wall. Curr Opin Microbiol **14:**698–703. http://dx.doi.org/10.1016/j.mib.2011.10.003.
42. **MacNeil DJ, Gewain KM, Ruby CL, Dezeny G, Gibbons PH, MacNeil T.** 1992. Analysis of *Streptomyces avermitilis* genes required for avermectin biosynthesis utilizing a novel integration vector. Gene **111:**61–68. http://dx.doi.org/10.1016/0378-1119(92)90603-M.
43. **Paget MS, Chamberlin L, Atrih A, Foster SJ, Buttner MJ.** 1999. Evidence that the extracytoplasmic function sigma factor SigE is required for normal cell wall structure in *Streptomyces coelicolor* A3(2). J Bacteriol **181:**204–211.
44. **Datsenko KA, Wanner BL.** 2000. One-step inactivation of chromosomal genes in *Escherichia coli* K-12 using PCR products. Proc Natl Acad Sci U S A **97:**6640–6645. http://dx.doi.org/10.1073/pnas.120163297.
45. **Redenbach M, Kieser HM, Denapaite D, Elchner A, Cullum J, Kinashi H, Hopwood DA.** 1996. A set of ordered cosmids and a detailed genetic and physical map for the 8 Mb *Streptomyces coelicolor* A3(2) chromosome. Mol Microbiol **21:**77–96. http://dx.doi.org/10.1046/j.1365-2958.1996.6191336.x.